ChemComm

COMMUNICATION

View Article Online
View Journal | View Issue

Cite this: *Chem. Commun.*, 2014, **50**, 3169

Received 3rd December 2013,
Accepted 6th January 2014

DOI: 10.1039/c3cc49176e

www.rsc.org/chemcomm

Highly stable covalent organic framework–Au nanoparticles hybrids for enhanced activity for nitrophenol reduction†

Pradip Pachfule,[a] Sharath Kandambeth,[a] David Díaz Díaz[bc] and Rahul Banerjee*[a]

Gold [Au(0)] nanoparticles immobilized into a stable covalent organic framework (COF) have been synthesized *via* the solution infiltration method. The as-synthesized Au(0)@TpPa-1 catalyst shows high recyclability and superior reactivity for nitrophenol reduction reaction than $HAuCl_4 \cdot 3H_2O$.

Covalent organic frameworks (COFs) are lightweight and porous materials well known for their applications in gas storage, catalytic supports, semiconductive and photoconductive devices.[1] In addition to other porous materials, *viz.* charcoal, dendrimers, polymers, mesoporous silica, zeolites, MOFs, *etc.*, metal doped COFs have also been practised as catalysts for organic reactions.[2] Although the well ordered periodicity and high surface area of COFs facilitated the usage of these materials as catalyst supports, the stability of host COF supports in aqueous–acidic–alkaline reaction media still remains a crucial aspect for using the same catalyst over a number of cycles.[3] Despite the limited surface area of COFs, nanoparticles@COFs have been used as catalyst for Suzuki coupling, C–H activation, Knoevenagel condensation, nitro reduction, glycerol oxidation, *etc.*[4] Since the COF based supports used to decorate the nanoparticles are unstable in aqueous and most of the organic solvents, tedious synthetic protocols are necessary for the synthesis as well as usage of these catalysts in the aforementioned reactions.[5] Moreover, the concerns regarding sintering, leaching, stability and recyclability of supported nanoparticles in diverse reaction conditions remain at the forefront.[6] Thus, in order to overcome these issues regarding the optimal interaction, we believe that the synthesis of new materials, having strong interactions between support and loaded nanoparticles with high stability in aqueous–acidic–alkaline media, is desired.

Gold (Au) nanoparticles decorated on suitable supports hold unique advantages as heterogeneous catalysts under mild conditions, even at ambient temperature with high reaction rates.[7] Although there are reports of host supported Au catalysts, which showed high catalytic activity for oxidations, hydrogenation, cyclization, rearrangement, C–C coupling reactions, *etc.*, the unstable supports holding these nanoparticles bring limitations to their uses.[8] Most importantly, the weak interactions between supports and nanoparticles usually result in the sintering and leaching of the nanoparticles. In these regards, Au catalysts supported on carbon, CeO_2, Al_2O_3, Fe_2O_3, *etc.*, have been used as catalysts for the hydrogenation of environmental pollutant 4-nitrophenol (4-NPh), which is anthropogenic, toxic and inhibitory in nature, to yield industrially important anilines like 4-aminophenol.[2a,8c] Since 4-aminophenol (4-APh) is important due to its usage as a developer in black and white films and as an intermediate for the synthesis of drug paracetamol, for its synthesis a catalytic system with high associated product yield, selectivity and recyclability is desirable. In order to simplify the modus operandi, herein for the first time, we report a simple synthetic route to acquire a highly stable, porous and crystalline COF (**TpPa-1**) supported Au nanoparticles hybrids *via* the solution infiltration method.[9] Herein, along with the synthesis of the robust and stable **Au(0)@TpPa-1** catalyst, the catalytic activities of synthesized catalyst towards 4-nitrophenol (4-NPh) reduction are illustrated.

As shown in Scheme 1, the **Au(0)@TpPa-1** catalyst was synthesized by mixing $\mathbf{HAuCl_4 \cdot 3H_2O}$ (1.5 mg, 0.004 mmol) with evacuated **TpPa-1** (50 mg) in 5 ml methanol under vigorous stirring.[9] From the obtained mixture, solvent was removed by evacuation and subsequently 3 ml methanol was added. To this solution, 2 ml of 0.5 mmol (20 mg) $NaBH_4$ solution in methanol was added wile stirring, and the obtained mixture was dried under vacuum after washing to obtain the **Au(0)@TpPa-1** catalyst (see the ESI,† Section S3). The consequential feature of the reported **Au(0)@TpPa-1** catalyst having high stability in aqueous and common organic solvents is associated with the proper selection of the support chosen as a stable COF (**TpPa-1**) having a well ordered porous architecture enriched with oxygen and nitrogen containing a crystalline framework, which provides extra strength to the nanoparticles. Here, the stability of synthesized

[a] *Physical/Materials Chemistry Division, CSIR-National Chemical Laboratory, Dr. Homi Bhabha Road, Pune 411008, India. E-mail: r.banerjee@ncl.res.in; Tel: +91 2025902535*

[b] *Institut für Organische Chemie, Universität Regensburg, Universitätsstr. 31, 93053 Regensburg, Germany*

[c] *IQAC-CSIC, Jordi Girona 18-26, 08034 Barcelona, Spain*

† Electronic supplementary information (ESI) available: Experimental procedures, IR, gas adsorption and additional supporting data. See DOI: 10.1039/c3cc49176e

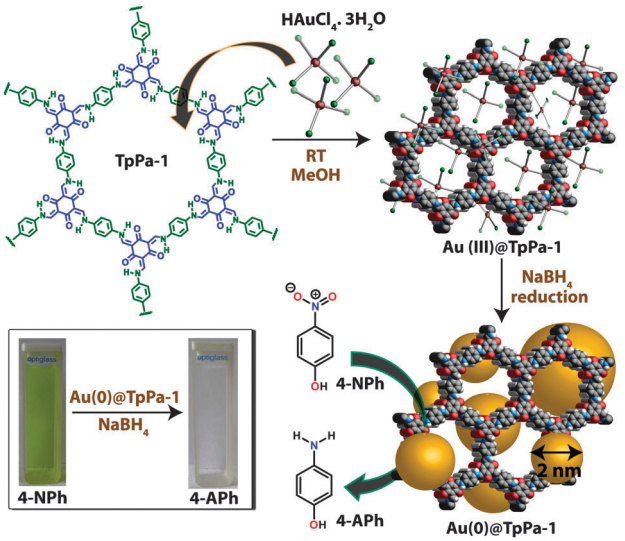

Scheme 1 Synthesis of the **Au(0)@TpPa-1** catalyst using the solution infiltration method for nitrophenol reduction reaction. Inset image: the optical images of the color change observed for the conversion of 4-nitrophenol to 4-aminophenol after the addition of **Au(0)@TpPa-1**.

catalyst was assumed to be optimal since the **TpPa-1** is stable in aqueous, acidic as well as alkaline media.

The well maintained PXRD patterns of **Au(0)@TpPa-1** with additional peaks for (111) and (200) planes appearing at ~39° (2θ) and ~44° (2θ) compared to **TpPa-1**, demonstrated the successful loading of Au nanoparticles with retention of the COF integrity and minimal loss of crystallinity, as shown in Fig. 1a. The presence of all the characteristics peaks of **TpPa-1** in the FT-IR spectrum of **Au(0)@TpPa-1** confirmed that, even after strong treatment with $NaBH_4$, the chemical

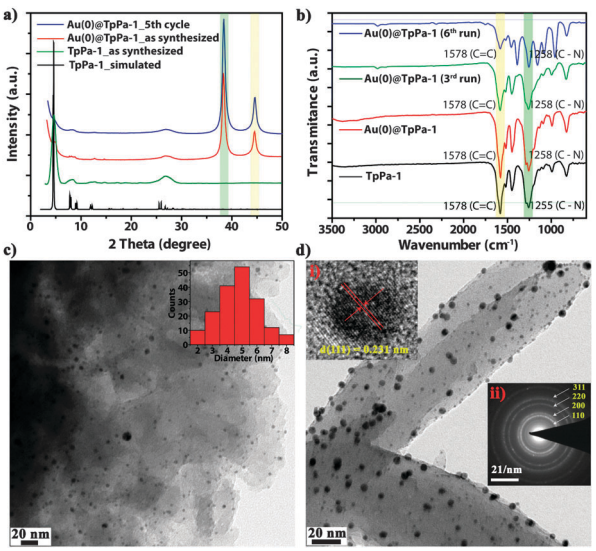

Fig. 1 (a) PXRD profile of **Au(0)@TpPa-1**. Matching PXRD plots of **TpPa-1**, **Au(0)@TpPa-1** and **Au(0)@TpPa-1** after 3rd and 5th catalytic cycle. (b) Comparison of the FT-IR spectra of **Au(0)@TpPa-1** with **TpPa-1**, catalyst recovered after 3rd and 6th run. (c) Low resolution TEM image of **Au(0)@TpPa-1**. Inset image: nanoparticles size distribution histogram. (d) High resolution TEM image of **Au(0)@TpPa-1**. Inset images: (i) single Au nanoparticle showing *d*-spacing, (ii) the corresponding SAED pattern.

composition within the COF framework remained intact (Fig. 1b). After incorporation of the Au(0) nanoparticles inside the **TpPa-1** template, the appearance of strong representative peaks for C=C (~1578 cm^{-1}) and the C–N (~1258 cm^{-1}) stretching of **TpPa-1**, confirmed the metal loading without disturbing the basic **TpPa-1** architecture. The complete reduction of Au(III) to Au(0) in presence of excess $NaBH_4$ was confirmed from the X-ray photoelectron spectroscopy (XPS) analysis (see the ESI,† Fig. S9). The extent of Au nanoparticle loading on **TpPa-1** was further confirmed by the decreased N_2 adsorption and BET surface area of **Au(0)@TpPa-1** (339 m^2 g^{-1}) in comparison with the as synthesized **TpPa-1** (484 m^2 g^{-1}). As the pore surface (partially or fully) and interlayer spacings in the host COF framework are occupied by finely dispersed Au(0) nanoparticles located at the surface as well as inside the COF matrix, the observed decrease in BET surface area and pore size is justified (see the ESI,† Fig. S7 and S8). From the EDAX, ICP and TGA analysis performed for **Au(0)@TpPa-1**, the loading of ~1.2 wt% Au nanoparticles on **TpPa-1** was confirmed (see the ESI,† Fig. S6 and S19).

As the morphological factors of the supported nanoparticles contribute to the actual reactivity and recyclability of the catalysts, we have performed SEM and TEM analyses on the synthesized catalyst.[10] The flower like morphology of the pristine **TpPa-1** was observed to be maintained to some extent even after the loading of Au(0) nanoparticles (see the ESI,† Fig. S2 and S4). The micrometer sized petals of **TpPa-1** observed in the SEM analysis were found to be the aggregation of the few sheet-like structures from the TEM analysis, which serves as host for the doped nanoparticles (Fig. 1d of the ESI,† Fig. S3). The loading of finely distributed 5 ± 3 nm sized Au(0) nanoparticles was clearly visible in the TEM analyses performed for **Au(0)@TpPa-1** (Fig. 1c), in concurrence with the particle size calculated from the observed PXRD patterns using the Scherrer equation. The 3D loading of these nanoparticles throughout the matrix of **TpPa-1** was clearly perceptible from the dark field TEM imaging of the **Au(0)@TpPa-1** (Fig. S5, ESI†). The interplanar *d*-spacing (0.231 nm) in the lattice fringes indicates the formation of Au(0) nanoclusters oriented in the (111) plane (Fig. 1d; inset i). The SAED pattern reveals the growth of nanocrystals with (200) and (220) orientations, with the presence of nanocrystalline texture in agreement with the observed XRD patterns (Fig. 1d; inset ii).

Since we have observed a uniform loading of 5 ± 3 nm sized Au nanoparticles on the **TpPa-1** matrix with a fine dispersion, we evaluated the kinetics as well as energetic parameters of the well known nitrophenol reduction reaction using the **Au(0)@TpPa-1** catalyst. In order to confirm the heterogeneity of the catalyst, we carried out a standard leaching experiment using the **Au(0)@TpPa-1** catalyst, which confirmed the stable loading of Au nanoparticles on **TpPa-1** in water as well as common organic solvents (see the ESI,† Fig. S16). The strong interaction of Au nanoparticles with **TpPa-1** proves that the heterogeneity of the catalyst remains intact in standard catalytic conditions. The as-synthesised **Au(0)@TpPa-1** were tested for the catalytic reduction of 4-NPh in the presence of excess $NaBH_4$ in water as the solvent. The reduction kinetics were monitored by UV-vis absorption spectroscopy of the reaction mixture after the addition of the catalyst. As the reaction proceed, the absorbance of 4-NPh at ~400 nm started decreasing along with a related increase in the ~300 nm peak corresponding to

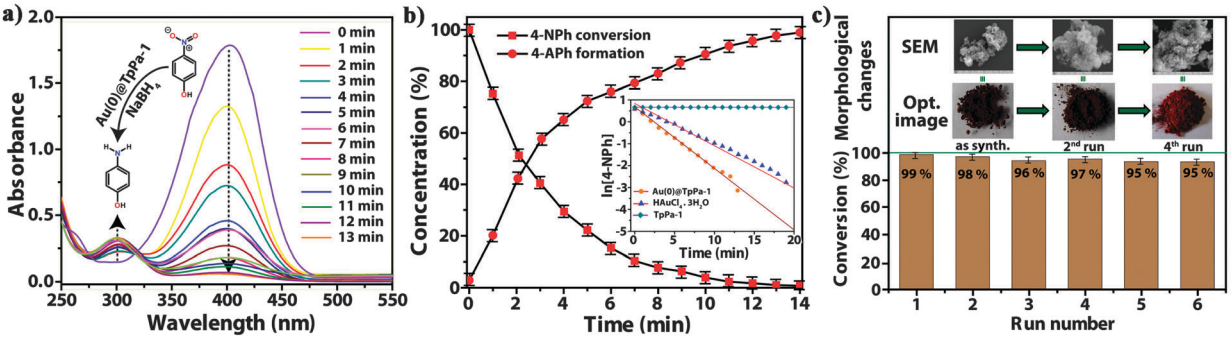

Fig. 2 (a) Typical time-dependent evolution of UV-vis spectra showing the catalytic reduction of 4-NPh to 4-APh by **Au(0)@TpPa-1**. (b) Kinetics of the reduction reaction of 4-NPh to 4-APh. Inset image: plots of the ln[4-NPh] absorbance of 4-nitrophenol at 400 nm obtained from (a) *versus* time for the reduction of 4-nitrophenol catalyzed by **Au(0)@TpPa-1**, **$HAuCl_4{\cdot}3H_2O$** and **TpPa-1**. (c) Conversion of 4-NPh during 6 cycles of reaction by the **Au@TpPa-1** catalyst. Inset image: morphological changes observed in the **Au(0)@TpPa-1** catalyst with an increasing number of cycles traced by optical imaging and SEM.

4-aminophenol (4-APh). The reaction did not occur when using only **TpPa-1** as the catalyst and proceeded comparatively slower with **$HAuCl_4{\cdot}3H_2O$** (conversion time: 20 min) and **Au(0)@TpPa-1** (2.20 wt%, conversion time: 18 min) as the catalysts (Section S4, ESI†). When 1.2 wt% Au loaded **Au(0)@TpPa-1** catalyst was used as the catalyst, a significant catalytic activity was observed and conversion of 4-NPh to 4-APh was completed within 13 min. The probable reason of the momentous activity shown by **Au(0)@TpPa-1** (1.20 wt%) over **Au(0)@TpPa-1** (2.20 wt%) may be the fine distribution of very tiny nanoparticles (5 ± 3 nm) on the **TpPa-1** matrix, which lead to a very large surface area of the nanoparticles and high particle number per unit mass for the catalyst. The increased fraction of the atoms at the surface in **Au(0)@TpPa-1** leads to a significantly higher catalytic activity.

In view of the fact that the concentration of BH_4^- added in the system is in excess compared to the concentration of 4-NPh, it is assumed that the concentration of BH_4^- remains constant during the reaction. Under this circumstance, pseudo-first-order kinetics have been used to evaluate the kinetic reaction rate of the catalytic reaction (Fig. 2b, inset). Herein, a linear correlation of ln[4-NPh] *versus* time at any instant is obtained. Among all the tested catalysts for the 4-NPh reduction, **Au(0)@TpPa-1** (1.20 wt%) has the highest activity with a rate constant of $\sim 5.35 \times 10^{-3}$ s^{-1}. The sluggish reaction kinetics in the presence of **$HAuCl_4{\cdot}3H_2O$** ($\sim 3.01 \times 10^{-3}$ s^{-1}) compared to than that of **Au(0)@TpPa-1** highlights the utility of supported nanoparticles for catalyzing organic transformation reactions heterogeneously (Fig. 2c). This catalytic activity is superior to the well known Au and Ag based catalysts tested under similar conditions (see the ESI,† Table S1).[11] Additionally, the catalyst has also showed excellent recyclability for more than 6 catalytic cycles giving yields over 95% in an estimated time span of 13 min. As calculated by the Arrhenius equation (Fig. S15, ESI†), the rate of 4-NPh reduction increased with temperature. The stability of the catalyst after catalytic cycles was furthermore confirmed by optical, SEM and TEM imaging of the catalyst recovered after catalytic runs (Fig. 2c inset of the ESI,† Fig. S17 and S18). The FT-IR and PXRD analyses of the reused catalyst once again highlights the stability and crystallinity of the COF support holding the nanoparticles intact even after 6 cycles (Fig. 1a and b). Moreover, as shown in the Fig. S14 (see the ESI†), the non-aggregation of nanoparticles in the reused catalyst further confirms the stability of the prepared catalysts. Hence, it can be confirmed that the prominent catalytic activity of **Au(0)@TpPa-1** might be assigned to the highly stable, two dimensional support (**TpPa-1**) which holds the loaded nanoparticles to a high extent.

In summary, for the first time, we have synthesized a COF-supported highly stable Au(0) based catalyst *via* solution infiltration methods, which shows a high activity towards nitrophenol reduction reaction. The synthesized **Au(0)@TpPa-1** catalyst shows superior reactivity for nitrophenol reduction reaction than **$HAuCl_4{\cdot}3H_2O$**, imparting the advantages of heterogeneous catalysts. The phenomenon of maintaining crystallinity over a number of cycles is very rare in the literature and herein we have demonstrated the usefulness of stable and crystalline supports for an improved catalytic activity. The overall recyclability with almost unchanged reactivity for more than 6 cycles shown by the reported catalyst is promising towards the heterogenization of Au catalysts for commercially important transformation reactions.

RB and PP acknowledges CSIR (CSC0102 and CSC0122) for funding.

Notes and references

1 (*a*) K. Sakaushi, E. Hosono, G. Nickerl, T. Gemming, H. Zhou, S. Kaskel and J. Eckert, *Nat. Commun.*, 2013, **4**, 1485; (*b*) M. Dogru and T. Bein, *Chem. Commun.*, 2013, DOI: 10.1039/c3cc46767h; (*c*) J. W. Colson and W. R. Dichtel, *Nat. Chem.*, 2013, **5**, 453; (*d*) X. Feng, X. Ding and D. Jiang, *Chem. Soc. Rev.*, 2012, **41**, 6010; (*e*) C. J. Doonan, D. J. Tranchemontagne, T. G. Glover, J. R. Hunt and O. M. Yaghi, *Nat. Chem.*, 2010, **2**, 235.

2 (*a*) A. Corma and H. Garcia, *Chem. Soc. Rev.*, 2008, **37**, 2096; (*b*) J. C. Fierro-Gonzalez and B. C. Gates, *Chem. Soc. Rev.*, 2008, **37**, 2127.

3 (*a*) S. Proch, J. Herrmannsdörfer, R. Kempe, C. Kern, A. Jess, L. Seyfarth and L. Senker, *Chem.–Eur. J.*, 2008, **14**, 8204; (*b*) T. Ishida, M. Nagaoka, T. Akita and M. Haruta, *Chem.–Eur. J.*, 2008, **14**, 8456.

4 (*a*) C. E. Chan-Thaw, A. Villa, P. Katekomol, D. Su, A. Thomas and L. Prati, *Nano Lett.*, 2010, **10**, 537; (*b*) S.-Y. Ding, J. Gao, Q. Wang, Y. Zhang, W.-G. Song, C.-Y. Su and W. Wang, *J. Am. Chem. Soc.*, 2011, **133**, 19816; (*c*) S. B. Kalidindi, K. Yusenko and R. A. Fischer, *Chem. Commun.*, 2011, **47**, 8506; (*d*) P. Zhang, Z. Weng, J. Guo and C. Wang, *Chem. Mater.*, 2011, **23**, 5243; (*e*) Y. Zhou, Z. Xiang, D. Cao and C.-J. Liu, *Chem. Commun.*, 2013, **49**, 5633.

5 (*a*) J. Long, H. Liu, S. Wu, S. Liao and Y. Li, *ACS Catal.*, 2013, **3**, 647; (*b*) S. B. Kalidindi, H. Oh, M. Hirscher, D. Esken, C. Wiktor, S. Turner, G. V. Tendeloo and R. A. Fischer, *Chem.–Eur. J.*, 2012, **18**, 10848.

6 P. Forzatti and L. Lietti, *Catal. Today*, 1999, **52**, 165.

7 (*a*) D. J. Cole-Hamilton, *Science*, 2003, **299**, 1702; (*b*) P. Hervés, M. Pérez-Lorenzo, L. M. Liz-Marzán, J. Dzubiella, Y. Lu and M. Ballauff, *Chem. Soc. Rev.*, 2012, **41**, 5577.
8 (*a*) F. Zaera, *Chem. Soc. Rev.*, 2013, **42**, 2746; (*b*) S. Schauermann, N. Nilius, S. Shaikhutdinov and H.-J. Freund, *Acc. Chem. Res.*, 2013, **46**, 1673; (*c*) A. Corma and P. Serna, *Science*, 2006, **313**, 332.
9 S. Kandambeth, A. Mallick, B. Lukose, M. V. Mane, T. Heine and R. Banerjee, *J. Am. Chem. Soc.*, 2012, **134**, 19524.
10 (*a*) A. T. Bell, *Science*, 2003, **299**, 1688; (*b*) M. S. Chen and D. W. Goodman, *Catal. Today*, 2006, **111**, 22.
11 (*a*) K. Hayakawa, T. Yoshimura and K. Esumi, *Langmuir*, 2003, **19**, 5517; (*b*) Y. Lu, Y. Mei, M. Drechsler and M. Ballauff, *Angew. Chem., Int. Ed.*, 2006, **45**, 813; (*c*) S. Jana, S. K. Ghosh, S. Nath, S. Pande, S. Praharaj, S. Panigrahi, S. Basu, T. Endo and T. Pal, *Appl. Catal., A*, 2006, **313**, 41; (*d*) J. Lee, J. C. Park and H. Song, *Adv. Mater.*, 2008, **20**, 1523.

